Knowledge E

enriching | engaging | empowering

Conference Paper

Thermal Treatment on MSWI Bottom Ash for the Utilisation in Alkali Activated Materials

Boyu Chen[1], Marc Brito van Zijl[2], Arno Keulen[2], and Guang Ye[1]

[1]Microlab, Section Materials and Environment, Faculty of Civil Engineering and Geosciences, Delft University of Technology, Stevinweg 1, 2628 CN Delft, The Netherlands
[2]Mineralz (part of Renewi), Waalwijk, The Netherlands

Abstract

At present, most municipal solid waste incineration (MSWI) bottom ash is directly landfilled, raising concerns about environmental issues and loss of resources. Due to its high mineral content, MSWI bottom ash is now being considered as a raw material to prepare alkali-activated materials (AAMs). However, the mineral fraction unavoidably contains metallic aluminium (Al) and zinc (Zn) scraps (<1 wt.%), which easily oxidise and generate H_2 gas under alkaline conditions. As a result, when using MSWI bottom ash to prepare AAMs, the formation of a porous structure as well as expansive cracks (both detrimental to strength development) can be observed. In this research, thermal treatment of MSWI bottom ash, at temperatures of 500 and 1000 °C, was performed to deal with the issue caused by metallic Al/Zn. A series of tests, including Quantitative X-ray diffraction (QXRD) analysis, fineness measurements (particle size and surface area), and the dissolution test, were conducted to examine the effects of thermal treatment on as-received bottom ash. The results indicate that it is difficult to oxidise metallic Al/Zn at 500°C, but heating up to 1000 °C can realize the complete oxidation of Al/Zn, which in turn allows the wide utilisation of bottom ash in AAMs.

Keywords: MSWI bottom ash, thermal treatment, alkali activated materials

OPEN ACCESS

1. Introduction

Incineration is regarded as one of the most efficient waste management practices to deal with the increasing amount of municipal solid waste (MSW). However, although incineration significantly decreases the demand for landfill [1, 2], the ever-increasing generation rate of municipal solid waste will inevitably intensify the pressure to landfill the incineration residue, consisting mainly of fly ash and bottom ash. Unlike municipal solid waste incineration (MSWI) fly ash, the recycling of MSWI bottom ash in building materials shows greater potential because it has stable leaching behaviour and accounts for 80-90% of the residue [3, 4]. Alkali-activated materials, usually synthesized at room temperature by using industrial wastes as raw materials, have been proved to be promising low-CO_2 emission alternatives to Portland cement [5]. Nowadays, there has

been much effort trying to use MSWI bottom ash for preparing AAMs [6-11]. But the compressive strength of alkali-activated MSWI bottom ash is usually very low (<5MPa) [11-13], due to the existence of residual metallic Al/Zn and the deficiency of reactive phases. It has been reported that thermal treatment can improve the quality of MSWI bottom ash from the viewpoint of reactivity enhancement and hazardous substance removal [11, 14]. Therefore, in this research, both low- and high-thermal treatments (500 or 1000°C) were performed on Fe-rich MSWI bottom ash to evaluate the effectiveness of this pre-treatment method on the oxidation of metallic Al/Zn and the promotion of reactive phase formation. For the bottom ash having the particle size smaller than 63 μm, 100% MSWI bottom ash based alkali-activated materials (AAMs) were prepared. Afterward, the mechanical properties of alkali-activated MSWI bottom ash were assessed to highlight the changes induced by thermal treatment.

2. Materials and Methodology

MSWI bottom ash with the particle size of 4-11mm was collected from a local waste-to-energy plant in the Netherlands. After a series of mechanical treatments mainly including pulverization and separation, low-metallic Al and Zn fraction with particle size smaller than 63μm was obtained and used as precursor to prepare alkali-activated materials. This type of bottom ash powder is called un-treated bottom ash (BA), as distinct from thermal-treated bottom ash. Thermal treatments were carried out in ceramic crucibles. The bottom ash was heated up to 500 or 1000 °C, then maintained at that temperature for 2 hours in muffle furnace under oxygen gas atmosphere. After calcination bottom ash was gradually cooled down to room temperature. The bottom ash heated at 500 and 1000 °C is named 500BA and 1000BA, respectively. Figure 1 illustrates the raw material used in this research.

Figure 1: Untreated and thermal-treated bottom ash.

Different characterization techniques were employed to identify the chemical and physical changes of bottom ash before and after thermal treatment. X-ray fluorescence (XRF) and X-ray diffraction (XRD) were used to determine the chemical and mineralogical

compositions, respectively. Quantitative analysis for XRD patterns was performed by the Rietveld method. For the sample preparation, ten percent (10 wt.%) of silicon powder was introduced as internal standard. A mixture of crystal structure model is selected to fit the observed pattern. The content of crystal phases can be determined by normalizing all patterns on an equal-silicon-intensity basis. The abundance of amorphous phase is calculated as the difference of the sum of the crystalline phases from 100%.

The metallic Al/Zn content in the bottom ash was calculated by measuring the gas volume generated upon its chemical reaction with NaOH solution. It is worth mentioning that both 500BA and 1000BA were ground to fine powders before the measurement of metallic Al/Zn. The particle size distribution of bottom ash was measured by the laser diffraction method (Malvern Mastersizer). The Brunauer-Emmett-Teller (B.E.T) test was used to determine the surface of bottom ash particles.

A dissolution test was conducted to reveal the potential alkali reactivity of BA and 500BA. This test was performed by following the method reported by Panagiotopoulou et al. [15], where 0.5 g bottom ash was submerged into 20 ml 4 M NaOH solution for 24 hours at room temperature. After that, the dissolved concentrations of trace elements (Si, Al, Ca, and Fe) in the filtered leachate were measured by ICP-OES.

A mixture of 4 M NaOH and Na_2SiO_3 solution, with SiO_2 to Na_2O molar ratio of 2.2, was used as alkali activator. The liquid to solid mass ratio was fixed at 0.5 for all mixtures. After 2 minutes mixing, the freshly prepared paste was cast into a mould with a dimension of 20 mm × 20 mm × 20 mm. The paste specimens, before de-moulding, were firstly cured at room temperature for 24 hours. Then cubic samples obtained were sealed with plastic bags and cured for another 6 and 27 days at 40 °C before compressive measurements. In total, two types of alkali-activated bottom ash, sorted by the name of bottom ash, were prepared. They are alkali-activated untreated bottom ash (AABA) and alkali-activated 500BA (AA500BA).

3. Results and Discussion

3.1. Chemical and Mineralogical Composition

In general, the changes in chemical composition induced by thermal treatment are minimal. As shown in Table 1, when comparing 1000BA, 500BA, and BA, there are only minor changes regarding the SiO_2, Fe_2O_3, and Al_2O_3 contents, while the CaO content changes within the deviation of the measurement. Apart from the commonly detected

main components, such as SiO_2, CaO, and Al_2O_3, Fe_2O_3 is also a major constituent of both un-treated and thermal-treated bottom ash (around 30 wt.%).

Regarding metallic Al/Zn content, 500BA contains almost the same amount of metal Al as BA, but no metallic Al/Zn was detected in 1000BA. These results indicate that the oxidation of metallic Al/Zn at low temperature is difficult, yet the high-temperature treatment has the potential to eliminate the volume expansion induced by the hydrogen gas release associated with the redox reaction of metallic Al/Zn in alkaline condition.

The unburned organic content in the untreated bottom ash is lower than 3 wt.%, which was measured at 500 °C by following the Dutch standard NEN-EN 1744-7:2010. It is worth mentioning that part of the weight loss caused by organic substance decomposition was compensated by the weight gain from the oxidation of ferrous iron during the ignition process. Therefore, this method is not suitable for Fe-rich bottom ash, and a more accurate method is needed.

TABLE 1: Chemical composition of untreated and thermal-treated bottom ash.

Elements (wt.%)	BA	500BA	1000BA
SiO_2	38.79	40.00	37.96
CaO	10.75	11.37	11.76
Fe_2O_3	28.77	28.93	31.09
Al_2O_3	7.15	8.41	8.10
Na_2O	3.27	3.99	3.91
K_2O	0.51	0.53	0.60
MgO	1.79	2.08	2.09
ZnO	0.47	0.50	0.55
PbO	0.09	0.08	0.08
Cr_2O_3	0.15	0.13	0.15
Cl	0.22	0.25	0.07
SO_3	0.60	0.83	0.69
Others	5.06	2.90	2.95
LOI_{500}	2.4	0	0
Metallic Al/Zn	0.14	0.13	0

As illustrated in Figure 2, there are significant differences in the mineralogical compositions of untreated and thermal-treated bottom ash. The BA is highly amorphous (66.6 wt.%), with quartz (SiO_2), diopside ($Fe_{0.31}Mg_{0.69}CaSi_2O_6$ or $Fe_{0.75}Mg_{0.25}CaSi_2O_6$) and magnetite being the main crystal phases, together with other phases including corundum (Al_2O_3), hematite (Fe_2O_3), gehlenite ($Ca_2Al_2SiO_7$), goethite (FeOOH), albite

($NaAlSi_3O_8$), wollastonite 1A ($CaSiO_3$), wustite (FeO), and calcite ($CaCO_3$). It is worth noticing that BA diffraction pattern also illustrates "hump" feature. A broad hump centred at a 2θ angle of 32.5 between 25 and 40°, albeit having low intensity, can be observed. This observation confirms the existence of the amorphous phase. The appearance of this hump can be attributed to the existence of post-consumer glass in BA.

The Fe detected in XRF analysis, either in the form of ferrous or ferric iron, mainly comes from magnetite, wustite, and hematite. Thermal treatment is accompanied by the iron oxidation reaction, from the ferrous to the ferric Fe. This oxidation corresponds to the phase transformation from magnetite and wustite in BA to hematite in 500 BA and 1000BA. As illustrated in Table 2, the decrease in the amount of wustite and magnetite is always accompanied by the increase in the quantity of hematite. The formation of hematite also reveals the reason for the colour change after thermal treatment: from brownish BA to reddish 500BA and 1000BA (as shown in Figure 1). In the diffraction pattern of 500BA, the peaks of magnetite overlap with that of hematite at some locations. Therefore, the peaks dominated by hematite are labelled as H(M). On the other hand, the peaks primarily contributed by magnetite are labelled as M(H).

Moreover, it was found that the 500°C heating subtly affected the mineralogical composition, excepting facilitating the iron oxidation and the decomposition of goethite. It is hard to detect the transformation from metallic Al and Zn to Al_2O_3 and ZnO from QXRD analysis, due to their very small amount.

When increasing the temperature to 1000 °C, calcite decomposition and glass melting occurred, followed by chemical reaction and phase transformation in the cooling process. As a result, the heat treatment leads to the formation of crystal phases such as diopside, Wollastonite1A, and andradite ($Ca_3Fe_2(Si_3O_{12})$). This phase transformation can be identified easily by comparing XRD patterns of 500BA and 1000BA. Compared with 500BA, in the diffraction pattern of 1000BA calcite peaks disappear, and the intensity of amorphous hump decreased dramatically, while peaks of newly formed crystals appear. Besides, the QXRD analysis also indicates the reduction of amorphous phase, from 66.6 wt.% in BA to 46.43 wt.% in 1000BA.

3.2. Particle Size and Surface Area

Particle size distribution and surface area strongly influence the reactivity of bottom ash. The particle size distributions of both untreated and treated bottom ash are illustrated in Figure 3. It can be seen that after thermal treatment, bottom ash particles become coarser than 10 μm. The 500BA has d_{50} of 31.1μm, almost two times the size of BA (16.96
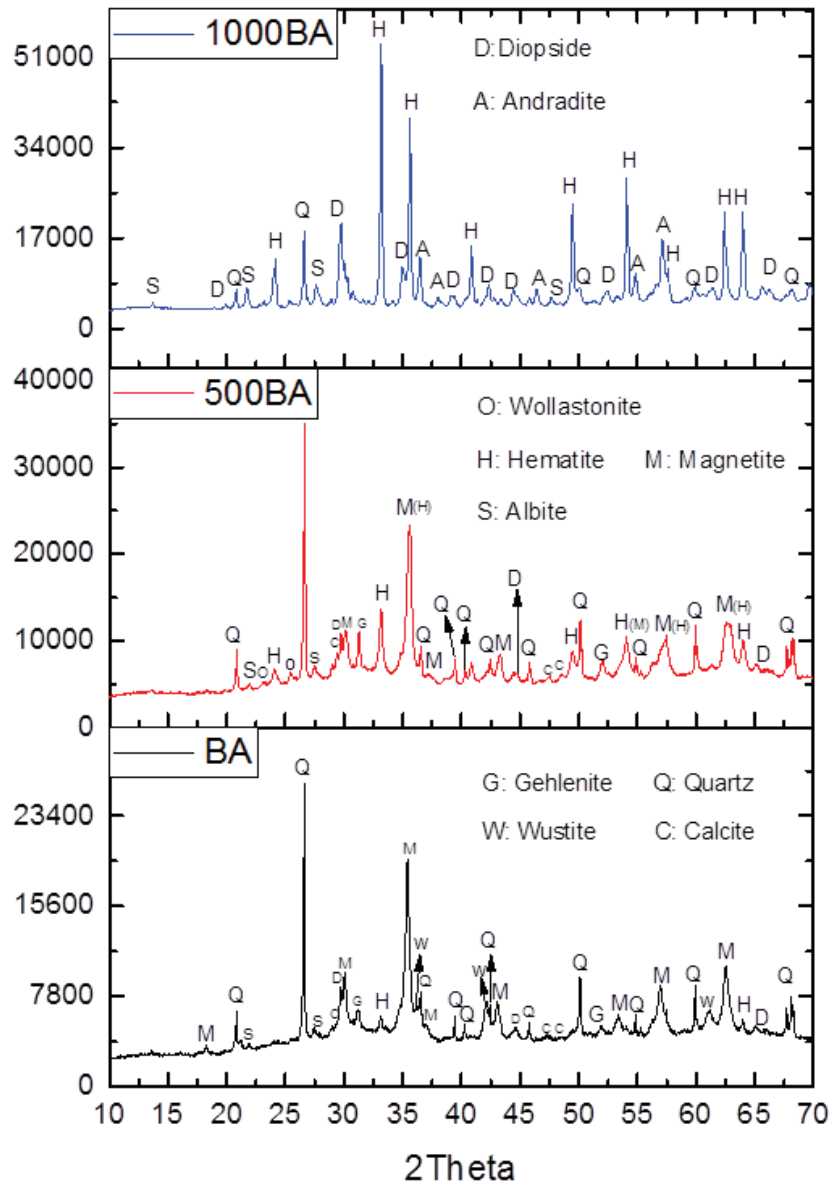
Figure 2: XRD pattern of untreated and treated bottom ash.

µm). But the particle size of 500BA is still smaller than 63 µm, which allows it to be used as binder materials. In contrast, the 1000BA (654.86 µm) has d_{50} more than 20 times of 500BA. The agglomeration of particles after thermal treatment is consistent with the phenomena observed by Qiao et al.[13].

The surface area of bottom ash particles decreases after thermal treatment. As shown in Table 3, the surface area of 500 BA and 1000BA particles is 25 % and 68 % smaller than that of BA, respectively. Since the amorphous content remains unchanged after thermal treatment at 500 °C, the electrostatic interaction might be the factor that causes the agglomeration of 500BA [14]. On the other hand, the surface

TABLE 2: Quantitative X-ray Diffraction analysis for un-treated and thermal-treated bottom ash.

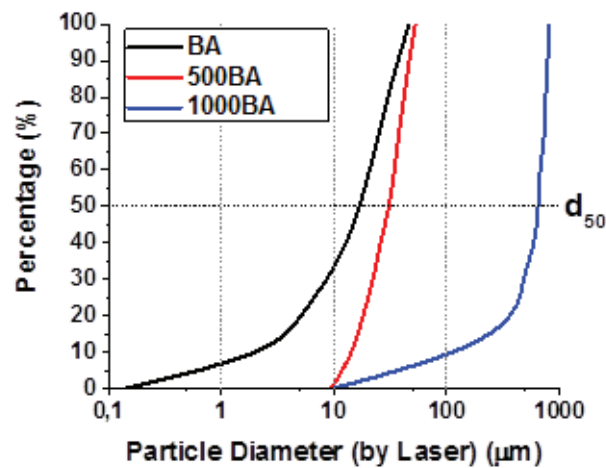| Phases (wt.%)	BA	500BA	1000BA
Corundum	0.86	1.03	0.82
Diopside	6.06	7.05	14.61
Iron	0.05	-	-
Hematite	0.97	4.82	16.60
Magnetite	5.35	4.28	0.12
Gehlenite	2.86	2.44	0.18
Goethite	1.50	0.38	-
Albite	1.74	2.49	2.34
Quartz	8.42	7.55	4.59
Wollastonite1A	2.28	1.98	5.26
Wustite	0.88	-	-
Calcite	2.43	1.63	-
Andradite	-	-	9.05
Amorphous	66.6	66.35	46.43

Figure 3: Particle size distribution of untreated and thermal-treated bottom ash.

area reduction after 1000 °C heating can be attributed to the melting of glass phases during the heating process, given that the amorphous content in 1000BA is less than that in BA (as illustrated in Table 2). The melted glass can cover the surfaces of its surrounding particles forming a dense layer, and at the same time, sticking particles together.

The particle agglomeration may help to prevent metallic Al/Zn from exposing to the alkaline solution. In the measurement of metallic Al/Zn content, the volume of hydrogen gas collected upon the alkaline dissolution of 500BA is similar to that from BA, but

TABLE 3: Surface area of untreated bottom ash and thermal-treated bottom ash.

Raw materials	BA	500BA	1000BA
Surface area (m^2/g)	4.20	3.13	1.33

hydrogen gas release was not detected in the test of 1000BA. It is highly possible that in 1000BA, the metallic Al/Zn was covered with the newly formed crystal phases such as diopside and andradite, which cannot dissolve in alkaline solution. Regarding 500BA, as no liquid phase formed after 500 °C thermal treatment, the physical bonding formed by electrostatic interaction might break when 500BA was immersed in alkaline solution.

3.3. Dissolution Behaviour

Dissolution tests were conducted to evaluate the alkali reactivity of both BA and 500BA. As illustrated in Table 4, the reactivity of bottom ash slightly decreased after 500 °C heating, with 20% less Si and 16% less Al dissolved from 500BA than that from BA. Unlike 1000BA, the reduction of the amount of the amorphous phase is not evident in 500BA relative to BA. Since the particle size will also influence the dissolution rate, the reactivity decrease of 500BA can be attributed to the increase of the particle size.

TABLE 4: Concentration of dissolved Si, Al, Ca, Fe from un-treated and thermal-treated bottom ash in the leachate (in ppm).

Dissolved elements (ppm)	BA	500BA
Si	168	134
Al	193	162
Ca	3.3	2.1
Fe	7.3	1.2

3.4. Compressive Strength

As can be seen in Table 5, the compressive strength of synthesized alkali-activated bottom ash is lower than 10 MPa. The 28-day strength of AABA and AA500BA is almost three times as high as 7-day strength. As mentioned above, the thermal treatment at 500 °C caused almost no change to the amorphous content of BA, but lead to the formation of bigger particles. Thus the alkali-activated materials prepared with 500BA are weaker than that with BA. The AA500BA has 28-day compressive strength 14 % lower than AABA. As shown in Figure 4. the volume expansion in AA500BA is more obvious than that of AABA. Considering that the metallic Al/Zn content in 500BA is

almost the same as that in BA, but 500BA released less amount of Si, Al, and Ca under alkaline condition, expansion cracks formed easily in AA500BA samples.

TABLE 5: Average 7- and 28-day compressive strength of alkali-activated pastes.

Compressive strength (MPa)	AABA	AA500BA
7-day	2.46 ±0.08	2.15 ±0.01
28-day	7.73 ±0.21	6.67 ±0.3
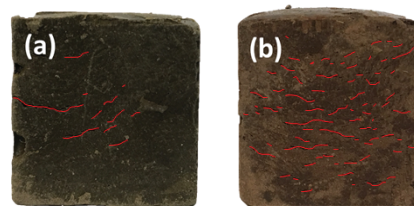
Figure 4: 28-day samples of alkali-activated bottom ash: (a) AABA; (b) AA500BA (the red lines represent the locations where cracks appear).

4. Conclusion

In the process of thermal treatment of Fe-rich MSWI bottom ash, ferrous iron present in the form of wustite or magnetite will transform into ferric iron in the form of hematite.

The high-temperature (1000 °C) thermal treatment conducted in this research could eliminate the detrimental effects induced by the existence of metallic Al/Zn via promoting particle agglomeration and non-alkali-reactive crystal phases formation to prevent the exposure of metallic Al/Zn in alkaline condition. In contrast, thermal treatment at 500 °C did little changes to the mineralogical composition and cannot oxidise the metallic Al/Zn present in bottom ash. The agglomeration occurred at 500 °C has adverse effects on the alkali-reactivity of bottom ash.

The slow cooling down procedure used in this thermal treatment is not beneficial to the formation of reactive phases. After thermal treatment, the bottom ash becomes more crystalline, accompanied by the loss of alkali-reactivity. The bottom ash obtained after 1000 °C heating is suitable for the application as fine aggregates provided that no further grinding is performed.

References

[1] Li, M., Xiang, J., Hu, S., et al. (2004). Characterization of solid residues from municipal solid waste incinerator. Fuel, vol. 83, no. 10, pp. 1397-1405.

[2] Sabbas, T., Polettini, A., Pomi, R., et al. (2003). Management of municipal solid waste incineration residues. Waste management, vol. 23, no. 1, pp. 61-88.

[3] Chimenos, J., Segarra, M., Fernández, M., et al. (1999). Characterization of the bottom ash in municipal solid waste incinerator. Journal of hazardous materials, vol. 64, no. 3, pp. 211-222.

[4] Lin, K., and Lin, D. (2006). Hydration characteristics of municipal solid waste incinerator bottom ash slag as a pozzolanic material for use in cement. Cement and Concrete Composites, vol. 28, no. 9, pp. 817-823.

[5] Provis, J.L., Duxson, P., and Van Deventer, J.S. (2007) J. Geopolymer technology and the search for a low-CO2 alternative to concrete. in:American Institute of Chemical Engineers Salt Lake City UT, United States

[6] Lancellotti, I., Cannio, M., Bollino, F., et al. (2015). Geopolymers: An option for the valorization of incinerator bottom ash derived "end of waste". Ceramics International, vol. 41, no. 2, Part A, pp. 2116-2123.

[7] Wongsa, A., Boonserm, K., Waisurasingha, C., et al. (2017). Use of municipal solid waste incinerator (MSWI) bottom ash in high calcium fly ash geopolymer matrix. Journal of Cleaner Production, vol. 148, pp. 49-59.

[8] Gao, X., Yuan, B., Yu, Q., et al. (2017). Characterization and application of municipal solid waste incineration (MSWI) bottom ash and waste granite powder in alkali activated slag. Journal of Cleaner Production, vol. 164, pp. 410-419.

[9] Lancellotti, I., Ponzoni, C., Barbieri, L., et al. (2013). Alkali activation processes for incinerator residues management. Waste Management, vol. 33, no. 8, pp. 1740-1749.

[10] Xuan, D., Tang, P., and Poon, C.S. (2018). MSWIBA-based cellular alkali-activated concrete incorporating waste glass powder. Cement and Concrete Composites.

[11] Qiao, X., Tyrer, M., Poon, C., et al. (2008). Characterization of alkali-activated thermally treated incinerator bottom ash. Waste management, vol. 28, no. 10, pp. 1955-1962.

[12] Chen, Z., Liu, Y., Zhu, W., et al. (2016). Incinerator bottom ash (IBA) aerated geopolymer. Construction and Building Materials, vol. 112, pp. 1025-1031.

[13] Qiao, X.C., Tyrer, M., Poon, C.S., et al. (2008). Novel cementitious materials produced from incinerator bottom ash. Resources, Conservation and Recycling, vol. 52, no. 3, pp. 496-510.

[14] Tang, P., Florea, M.V.A., Spiesz, P., et al. (2016). Application of thermally activated municipal solid waste incineration (MSWI) bottom ash fines as binder substitute. Cement and Concrete Composites, vol. 70, no. Supplement C, pp. 194-205.

[15] Panagiotopoulou, C., Kontori, E., Perraki, T., et al. (2007). Dissolution of aluminosilicate minerals and by-products in alkaline media. Journal of Materials Science, vol. 42, no. 9, pp. 2967-2973.